Intensively Computational Electromagnetic Tecniques for the Analysis of Complex Communication Devices

F. D. Quesada-Pereira, J. Pascual-Garcia, D. Cañete-Rebenaque, J.L. Gomez-Tornero, and A. Alvarez-Melcon,

***Abstract*— In this paper we introduce several formulations for the analysis of complex electromagnetic problems, based on the Integral Equation technique. The formulations are introduced in order to establish their advantages and drawbacks, as related to the application of advanced parallel computational techniques. The first formulation uses a very simple Kernel in the integral equation. This approach leads to huge systems of linear equations, which must be solved efficiently. In the second formulation, a complex Kernel is formulated to incorporate some features of the structure. In this way, the final numerical solution of the problem is reduced, and smaller systems of linear equations must be inverted. In this case the computational effort must be focused in the calculation of millions of smaller problems. Both formulations are applied to the analysis and study of practical communication devices, showing the need to develop powerful computational techniques.**

***Index Terms*— Integral Equation, Spatial Images, Green's functions**

I. INTRODUCTION

IN telecommunication engineering, it is very important to be able to design complex devices to be incorporated to the future communication systems. Due to the increasing complexity of the next generation of communication systems, the development of efficient computer aided design (CAD) tools is essential, in order to reduce development time and cost [Delhote et al., 2007]. If accurate computer models are available, the costly experimental tasks in the laboratory can be considerably reduced and minimized.

On the other hand, the analysis of complex systems is difficult, and often requires huge resources in terms of computational time and memory usage. In this sense, the optimization of complex devices usually involves hundreds of time consuming analysis. This situation makes impractical the use of many CAD tools for the design of real communication devices. For the development of useful CAD tools in the telecommunication sector it is indispensable to reduce computational time and cost. Only in this case it will be possible to accomplish the design of complex devices in real time.

For the solution to the efficiency problem, currently there are two possible solutions, which in many cases should be complementary. The first one is to develop new algorithms and techniques, which can solve a specific problem in a more efficient way, reducing the numerical overload. For this to be possible, it is often needed to apply inventiveness, and to push the analytical possibilities of the problem to a maximum. In this case, mathematical transformations to simplify the original problem might prove useful. An example are, for instance, transformations to accelerate the convergence of series, or of improper integrals.

The second approach to the efficiency problem goes through the use of faster and more powerful computers. In this case, the utilization of parallel computational algorithms can considerably improve the time performance. This is because some computations can be split among the different processors of the computer, and they can be executed in parallel. Also, the investigation of new algorithms to invert more efficiently large systems of linear equations, or the utilization of more powerful iterative solvers, can be useful.

Following the above ideas, in this contribution we present two different approaches to the analysis of complex communication devices using the integral equation technique. Both techniques are computationally very intensive for complex structures, but intrinsically they are very different. Therefore, different solutions to the efficiency problem might apply to them. The first technique formulates the Kernel of the integral equation using the free-space Green's functions. Following this approach, the Kernel contains very little information on the structure to be analyzed. Therefore, the numerical treatment of the problem must be extended to the whole structure, leading to large systems of linear equations.

In the second approach we formulate a more elaborated Kernel. Following analytical and numerical techniques, it is possible to formulate a complex Kernel that takes into account the shielding enclosure of the device, and the dielectric substrates of the microstrip circuits. Therefore, the numerical treatment of the problem is reduced to only the printed metallizations of the circuit. Following this approach, the overall problem is split into many smaller problems. The most suitable computational techniques to treat this second approach might (probably) be of very different nature, as compared to the first formulation.

II. THEORY

In this section we review two different approaches for the formulation of integral equation techniques, applied to shielded microstrip circuits. We point out the differences between them with respect to the numerical effort required for their solution.

Technical University of Cartagena, Campus Muralla del Mar s/n, Cartagena, E-30202, Spain, E-mail: fernando.quesada@upct.es.

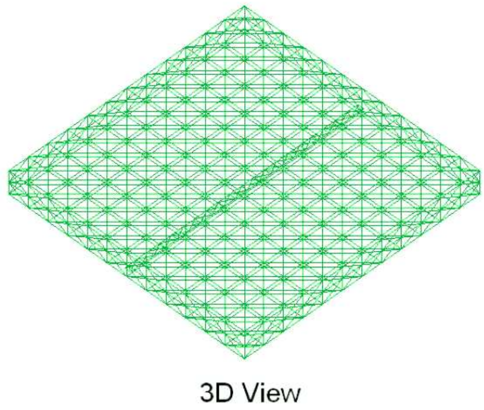

Fig. 1. Numerical treatment of a shielded microstip line using a free-space integral equation model.

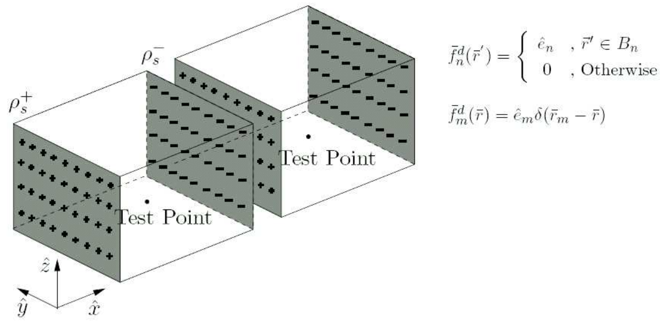

Fig. 2. Example of basis functions defined in hexahedral cells for volumen discretizations.

A. Integral equation based on free-space Kernel

The analysis of complex communication devices following the integral equation technique can be accomplished with the so-called free-space Kernel. In this case the Kernel is very simple in form, involving only complex exponentials, as follows:

$$\overline{\overline{G}}_A(\bar{r}, \bar{r}^{'}) = \frac{\mu_0\, e^{-jk_0|\vec{r}-\vec{r}\,'|}}{4\pi\,|\vec{r}-\vec{r}\,'|} \qquad (1)$$

where $(\vec{r}\,')$ denotes the position of a source point, $(\vec{r})$ is the point where the potential is evaluated, and k_0 is the propagation constant of a wave in free-space.

Once the Kernel is known, the integral equation technique proceeds with the imposition of the boundary conditions for the fields at the surfaces of the structure. These boundary conditions are imposed numerically on average on these surfaces (or volumes), using a geometrical spatial discretization with rectangular or triangular cells [Rao et al., 1982]. The simple Kernel formulated in equation (1) only has information on the radiation condition of the fields at the infinity. No other information of the geometry is contained in the formulated Kernel. Consequently, the boundary conditions for the fields at all surfaces of the structure need to be numerically imposed. This process requires the discretization of the whole structure, in order to numerically impose the appropriate boundary conditions. As an example, we present in Fig. 1 the discretization performed on a shielded microstrip line using triangular cells. It can be observed in the figure that all surfaces of the structure are discretized, including the shielding box.

Another important aspect to be considered, is that the simple Kernel formulated does not contain any information on dielectric objects. Consequently, the boundary conditions for the fields must also be imposed on the dielectric substrates used to print microstrip circuits. In this case, the appropriate boundary conditions can be enforced using either volume or surface formulations [Peterson et al., 1998]. If volume formulations are used, then the whole volume of the dielectric objects need to be discretized using volumetric subsectional basis functions. An example of such volumetric basis functions is given in Fig. 2. It can be seen that in this case, the basis functions are defined on hexahedral cells for the discretization of the whole volume. More elaborated definitions on tetrahedral cells are also possible [Schaubert et al., 1984]. If, on the contrary, surface formulations are used, then again the whole surface of the dielectric objects need to be discretized as shown in Fig. 1.

In any case, it is simple to see that this integral equation technique rapidly leads to the formulation of huge systems of linear equations, as soon as the complexity of the structure increases. Following this approach, then, the bottleneck from the efficiency point of view is the solution of huge systems of linear equations.

B. Using more complex Kernels

In order to reduce the size of the linear systems formulated with the previous approach, one possibility is to formulate more complex Kernels. The idea is to include automatically, inside the Kernel, the boundary conditions for the fields at some of the surfaces of the structure under study. Then, the numerical treatment of the problem is reduced to the imposition of the boundary conditions at the rest of the surfaces not included in the Kernel.

One immediate example can be considered, when a microstrip circuit is shielded with a rectangular cavity. For this structure, a more advanced Kernel can be formulated by including the effects of the lateral walls of the cavity inside the Green's functions. For the case of a rectangular cavity, the Kernel can be formulated quasi-analytically in the form of infinite series [Park and Nam, 1997]:

$$G_{Spec}^{(ext)}(x, x', z-z') = \frac{2}{a\,\pi} \sum_{n=0}^{\infty} \tilde{G}(k_x, z-z')\, f_n(k_x\, x)\; g_n(k_x\, x') \qquad (2)$$

where f_n and g_n are sinusoidal functions.

The main problem of this approach is the very slow convergence behavior of the series used to represent the Kernel. This slow convergence behavior makes, in general, impractical this approach. However, mathematical transformations are still possible in order to accelerate the convergence of this series. Two transformations very popular are the Kummer [Leviatan et al., 1983] and the Ewald [Capolino et al., 2005] techniques. As an example, we give in Fig. 3 the convergence

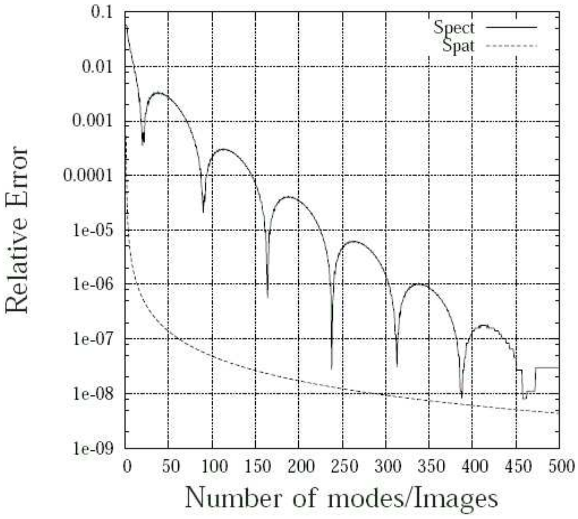

Fig. 3. Convergence behavior of the spectral series after application of the Kummer technique.

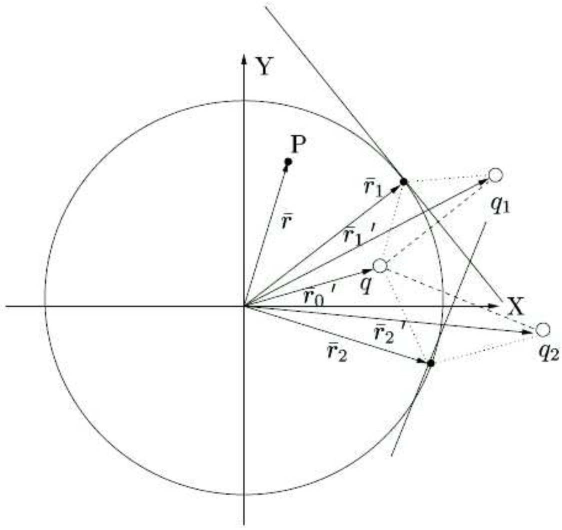

Fig. 4. Spatial images used to enforce the boundary condition for the electric scalar potential.

behavior of the series after application of the Kummer technique. We observe that about 100 terms in the series are needed to obtain a relative error of (10^{-4}). This convergence result shows that the calculation of the Kernel following equation (2) can be time consuming.

The problem of formulating more intelligent Kernels in the integral equation becomes complicated, when the shape of the cavity is different than the rectangular one. For those cavities, analytical expressions of the type of equation (2) simply do not exist. In these cases we seem to be trapped with the free-space Kernel, leading to huge systems of linear equations. Recently, however, a new formulation based on spatial images has been proposed for the calculation of integral equation Kernels in complex shaped cavities [Castejon et al., 2004]. The technique was first developed to treat circular cavities [Pereira et al., 2005], and it was latter extended for arbitrarily shaped cavities [Diaz et al., 2007].

Basically, the technique consist of placing spatial images around the cavity. These images are used to impose the boundary conditions for the fields at discrete points along the cavity wall. In Fig. 4 we show the basic concept for the electric scalar potential inside a circular cylindrical cavity. The imposition of the boundary conditions for the electric scalar potential leads to a system of linear equations of the following form:

$$\sum_{k=1}^{N} q_k \, G_V(\bar{r_i}, \bar{r_k}') = -G_V(\bar{r_i}, \bar{r_0}'); \quad i = 1, 2, \cdots, N \quad (3)$$

From this system we can compute the N-image charges (q_k) needed to satisfy the right boundary conditions at N-points along the cavity wall.

For the magnetic vector potential we can proceed in a similar way. However, in this case we need to take into account for the vector nature of the magnetic potential. This vector nature splits the boundary conditions in two components, one normal and the other tangent to the cavity wall. To be able to

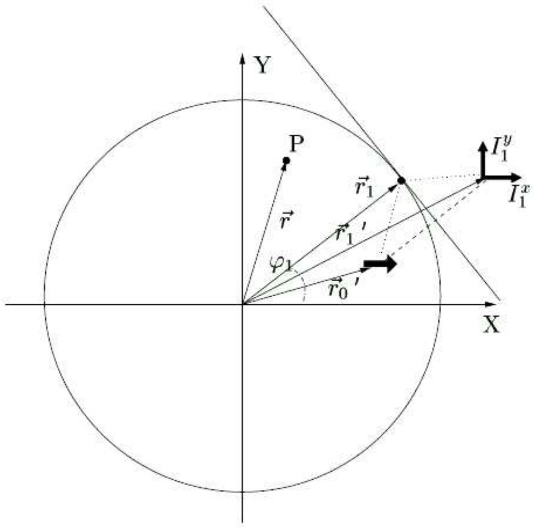

Fig. 5. Dipole image used to enforce the boundary conditions for the magnetic vector potential. Boundary conditions for the normal and tangent components are imposed by adjusting both the strength and the orientations of the image dipoles.

impose both conditions, we propose to use image dipoles with orientations. Following this approach, we can calculate both, the strength of each dipole and the orientation, in order to fulfill both boundary conditions at the same time. The basic idea is illustrated in Fig. 5 for a circular cylindrical cavity. The whole process leads to a system of linear equations with double size as compared to the previous one, namely:

$$-\sin(\varphi_i) \sum_{k=1}^{N} G_A^{xx}(\bar{r_i}, \bar{r_k}') \; I_k^x + \cos(\varphi_i) \sum_{k=1}^{N} G_A^{yy}(\bar{r_i}, \bar{r_k}') \; I_k^y = \sin(\varphi_i) \; G_A^{xx}(\bar{r_i}, \bar{r_0}') \quad (4a)$$

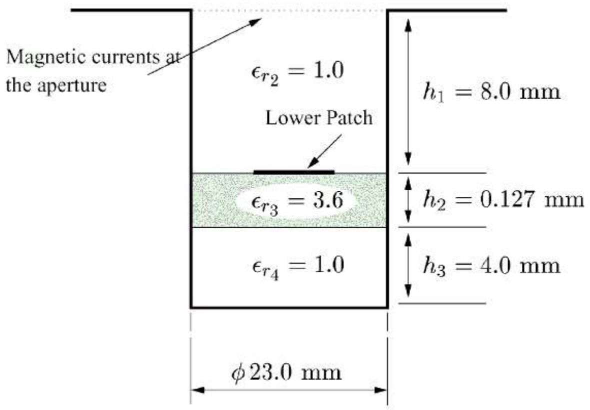

Fig. 6. Cavity antenna printed on a suspended substrate.

$$+\cos(\varphi_i)\sum_{k=1}^{N} C_{i,k}^{x}\; I_k^x + \sin(\varphi_i)$$
$$\sum_{k=1}^{N} C_{i,k}^{y}\; I_k^y = -\cos(\varphi_i)\; C_{i,0};\quad i = 1, 2\cdots N \tag{4b}$$

where we have defined the following constants:

$$C_{i,k}^{x} = \frac{G_A^{xx}(\bar{r_i}, \bar{r_k}')}{\rho} + \hat{e}_\rho \cdot \nabla G_A^{xx}(\bar{r_i}, \bar{r_k}') \tag{5a}$$

$$C_{i,k}^{y} = \frac{G_A^{yy}(\bar{r_i}, \bar{r_k}')}{\rho} + \hat{e}_\rho \cdot \nabla G_A^{yy}(\bar{r_i}, \bar{r_k}') \tag{5b}$$

Following this approach, we have to solve two systems of linear equations of sizes (N) and $(2N)$, for each position of the source point inside the cavity. These systems of linear equations are in general of small size. We have verified that only five points per wavelength of the perimeter are required to achieve good convergence. Therefore, the linear systems to be solved rarely exceeds the dimensions of $N = 15$ to $N = 25$.

In addition to above formulation, the analytical possibilities of the problem can be pushed to a maximum by including in the Kernel the dielectric layers using the Sommerfeld formalism [Felsen and Marcuvitz, 1973]. In this case the relevant Green's functions are computed analytically in the spectral domain. They are finally calculated in the spatial domain with an inverse Fourier transformation (Sommerfeld integrals). The great advantage of this technique, is that substrate layers of microstrip circuits can be included automatically in the Kernel of the integral equation. Therefore, they do not have to be considered during the numerical solution of the problem, avoiding complex volume or surface discretizations.

Following these quasi-analytical techniques, we have managed to spread the computational burden of the problem between several elements of the formulation. In fact, since the cavity walls and the dielectric layers are already inside the Kernel, the boundary conditions for the fields must be numerically imposed only on the printed metalizations. As an example we show in Fig. 6 a cavity antenna printed in a multilayer structure. All the elements of the antenna are included in the Kernel of the integral equation (cavity, and dielectric substrates). Consequently, only the printed patch on top of the substrate need to be numerically treated during the imposition of the boundary conditions. In this example, the radiating patch contains a complex circular structure to produce waves with circular polarization. The discretization of the radiating patch using triangular cells is shown in Fig. 7. Even-though the shape of the patch is complex, the final system of linear equations that we formulate with this technique can be rather small. However, the bottleneck in the efficiency issue is now moved to the fast calculation of the integral equation Kernel. For rectangular cavities, we need to perform the summation of the involved series millions of times, for each combination of source-observer points. For the case of the spatial images technique we need to solve hundreds of small systems of linear equations, one for each position of the source point inside the cavity.

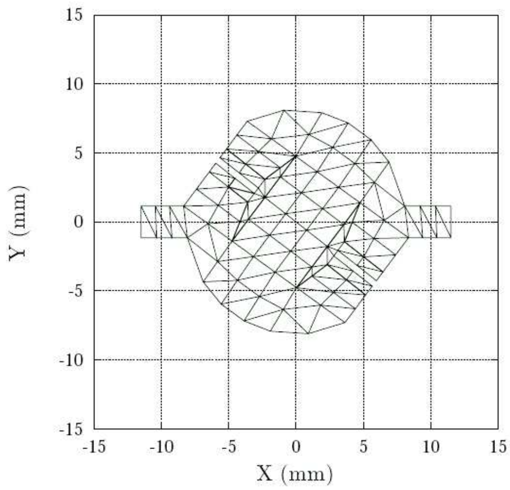

Fig. 7. Discretization of a radiating patch for circular polarization.

III. RESULTS

In this section we are going to include some application examples to show the usefulness of the formulations presented for the analysis of practical communication devices. Although the techniques presented are accurate, the optimization of the computational times will be important for the final development of useful CAD tools. Consequently, the incorporation of parallel computational techniques is desirable.

The first example that we treat is a microwave bandpass filter composed of microstrip line resonators, as shown in Fig. 8. For this structure, the analytical possibilities of the problem can be used to formulate a complex Kernel in the form of slow convergent series. Alternatively, the spatial images technique previously described can also be used to model the cavity. In both cases, the results obtained with the different formulations agree very well, as shown in Fig. 9

The next example is the cavity backed antenna presented in Fig. 6 and Fig. 7. In this case we present in Fig. 10 the results obtained inside a rectangular cavity using the slowly convergent series. The results obtained with the spatial images technique applied to a circular cavity are also included. Finally, these results are compared with measured results showing the

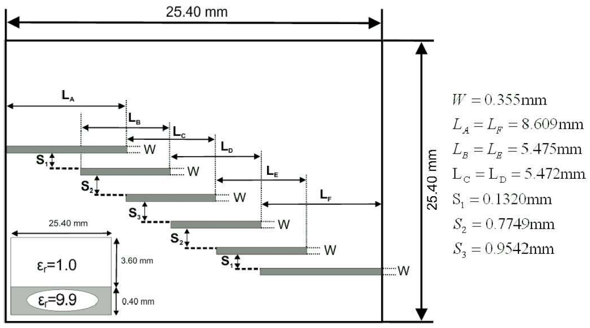

Fig. 8. Geometry of a shielded microstrip bandpass filter based on microstrip line resonators.

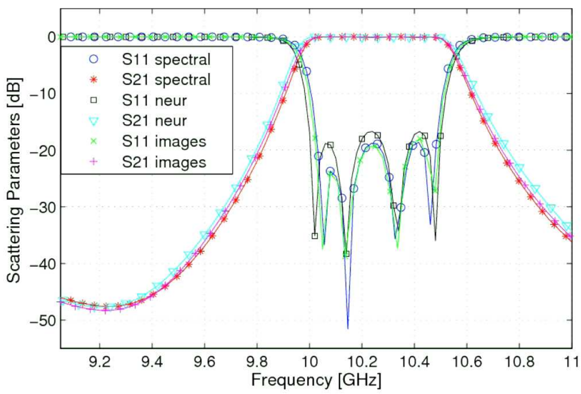

Fig. 9. Results for the filter shown in Fig. 8, using different integral equation formulations.

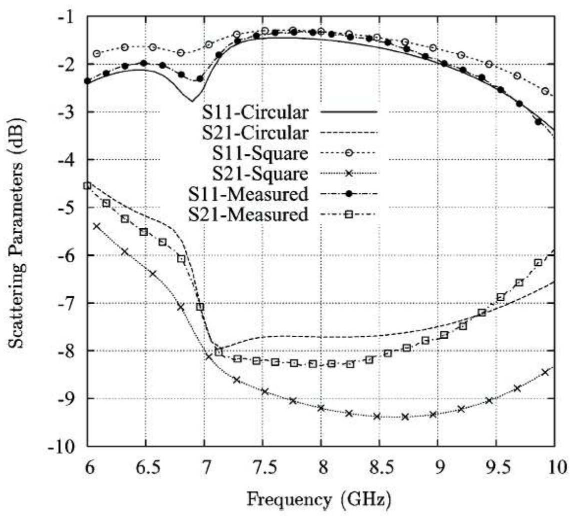

Fig. 10. Measured and simulated results for the cavity backed antenna presented in Fig. 6 and Fig. 7.

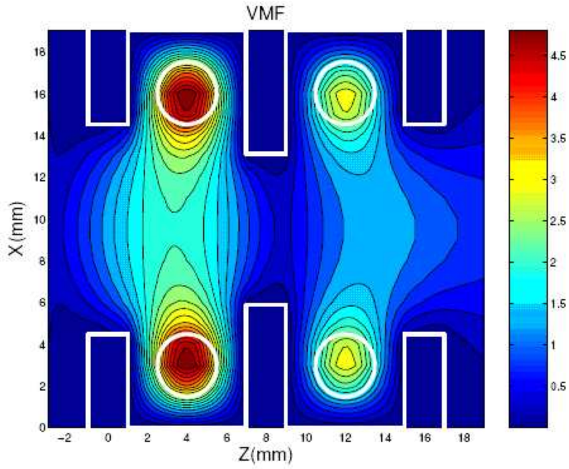

Fig. 11. Electric field distribution in a waveguide filter. Dielectric posts are used to produce a more uniform field at the center of the resonators. Radius of dielectric posts $R = 1.5$ mm, $\epsilon_r = 10$

accuracy of the different techniques. In particular, we observe from the results that the circular cavity model agrees better with the measured results. This is because the breadboard in this case was manufactured using a circular cavity. The example shows the importance to model accurately the shape of the cavity to obtain precise results.

The last example that we treat is the calculation of the electromagnetic fields in order to investigate radio-frequency (RF) breakdown phenomena [Vicente et al., 2005]. With the techniques presented, it is possible to calculate the electromagnetic fields inside complex communication devices. For high power applications, these devices might suffer from RF-breakdown effects, such as multipactor or corona. The tools presented can be used to investigate the risk of these unwanted effects, and to explore alternatives to mitigate the consequences. An example is given in Fig. 11, where we present a waveguide microwave filter with dielectric posts placed off-centered inside the cavity resonators. The pulling effect introduced by the dielectric posts is able to produce a more uniform field distribution inside the center of the cavity. This effect leads to a reduction of RF-breakdown risk in about 20% with respect to the original design. A stronger behavior can be obtained if the pulling effect is introduced more gently at the center of the cavity. This can be implemented by using dielectric posts with triangular shape. One of the vertex of the triangle will be placed close to the center of the cavity, to obtain a more gentle pulling effect. The electric field in this situation is presented in Fig. 12. It has been observed that the RF-breakdown risk has been reduced by about 30% with respect to the original design.

IV. Conclusions

In this contribution we have outlined several formulations for the analysis of shielded microstrip circuits using the integral equation technique. During the presentation we have pointed out the important aspects of each formulation, that have strong impact on the computational efficiency. First we

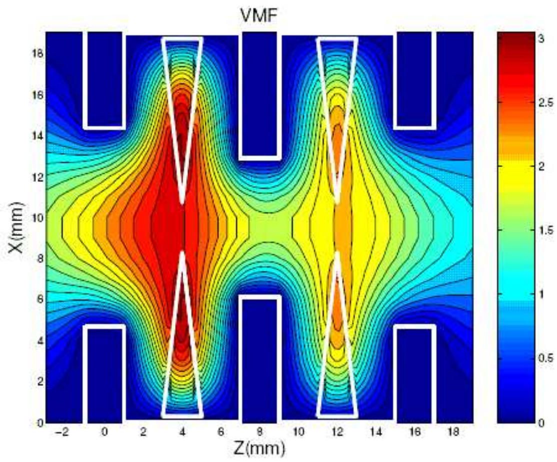

Fig. 12. Electric field distribution in the same waveguide filter as before, but using triangular dielectric posts.

have introduced the basic formulation using the free-space Kernel. Since this Kernel is very simple, it contains very little information of the structure, and the numerical treatment leads to huge systems of linear equations. Following this approach, the effort should be concentrated in developing efficient algorithms to invert very large systems of linear equations. Alternatively, we can formulate integral equations with more complex Kernels. These Kernels already contain information of the shielding cavity and of the substrate layers. Therefore, the numerical treatment of the problem is reduced to only the printed metalizations. Following this approach, the final system of linear equations is small. However, the effort should now be concentrated in the solution of hundreds or even millions of small problems, needed for the evaluation of the Kernel for every source-observer combination. Although the results obtained following both approaches are accurate, the intrinsic differences between them may lead to very different strategies in order to increase the computational efficiency. The collaboration between research groups to work towards the incorporation of parallel computational techniques to the basic formulations, is very much desirable. This may lead to the development of useful CAD tools for the Telecommunication industry.

References

[Capolino et al., 2005] Capolino, F., Wilton, D. R., and Johnson, W. A. (2005). Efficient computation of the 2-D Green's function for 1-D periodic structures using the Ewald method. IEEE Transactions on Antennas and Propagation, 53(9):2977–2984.

[Castejon et al., 2004] Castejon, P. V., Pereira, F. Q., Rebenaque, D. C., Garcia, J. P., and Melcon, A. A. (2004). Numerical evaluation of the Green's functions for cylindrical enclosures by a new spatial images method. In IEEE MTT-S International Microwave Symposium Digest, Fort Worth, Texas, USA. No. TH5A-6.

[Delhote et al., 2007] Delhote, N., Baillargeat, D., Verdeyme, S., Delage, C., and Chaput, C. (2007). Ceramic layer-by-layer stereolithography for the manufacturing of 3-D millimeter-wave filters. IEEE Transactions on Microwave Theory and Techniques, 55(3):548–554.

[Diaz et al., 2007] Diaz, J. G., Mendoza, M. M., Pereira, F. Q., Garcia, J. P., Soler, F. P., and Melcon, A. A. (2007). Numerical evaluation of the Green's functions for arbitrarily shaped enclosures. In IEEE MTT-S International Microwave Symposium Digest, Honolulu, Hawaii, USA. IEEE. No. THP1B-01.

[Felsen and Marcuvitz, 1973] Felsen, L. B. and Marcuvitz, N. (1973). Radiation and Scattering of Waves. Prentice-Hall. New Jersey, USA.

[Leviatan et al., 1983] Leviatan, Y., Li, P. G., Adams, A. T., and Perini, J. (1983). Single post inductive obstacle in rectangular waveguide. IEEE Transactions on Microwave Theory and Techniques, 31(10):806–812.

[Park and Nam, 1997] Park, M.-J. and Nam, S. (1997). Rapid calculation of the Green's function in the shielded planar structures. IEEE Microwave and Guided Wave Letters, 7(10):326–328.

[Pereira et al., 2005] Pereira, F. Q., Castejon, P. V., Rebenaque, D. C., Garcia, J. P., and Melcon, A. A. (2005). Numerical evaluation of the Green's functions for cylindrical enclosures. IEEE Transactions on Microwave Theory and Techniques, 53(1):94–105.

[Peterson et al., 1998] Peterson, A. F., Ray, S. L., and Mittra, R. (1998). Computational Methods for Electromagnetics, page 451. IEEE Press.

[Rao et al., 1982] Rao, S. M., Wilton, D. R., and Glisson, A. W. (1982). Electromagnetic scattering by surfaces of arbitrarily shape. IEEE Transactions on Antennas and Propagation, 30(5):409–418.

[Schaubert et al., 1984] Schaubert, D. H., Wilton, D. R., and Glisson, A. W. (1984). A tetrahedral modeling method for electromagnetic scattering by arbitrarily shaped inhomogeneous dielectric bodies. IEEE Transactions on Antennas and Propagation, 32(1):77–85.

[Vicente et al., 2005] Vicente, C., Mattes, M., Wolk, D., Hartnagel, H., Mosig, J., and Raboso, D. (2005). FEST3D - a simulation tool for multipactor prediction. In International Workshop on Multipactor, Corona and Passive Intermodulation in Space RF Hardware, Noordwijk, The Netherlands. ESA/ESTEC.